

Fabricating Suspended Carbon Wires Using SU-8 Photolithography

E. Giogli^a, M. Islam^a, and R. Martinez-Duarte^a

^aDepartment of Mechanical Engineering, Clemson University, Clemson, South Carolina 29634, USA

We present initial results towards the fabrication of suspended structures between photo-patterned high aspect ratio SU-8 posts as precursors for carbon wires and bridges. Initial results show that carbon wires of diameter as low as 800 nm can be formed. SU-8 is an epoxy-based negative photoresist, commonly used as high quality carbon precursor in carbon MEMS technology. This work has two main goals: 1) characterize the formation of suspended structures between SU-8 posts depending on the photolithography exposure setup and time of the exposure, the shape and size of the anchors and the gap between them; and 2) examine the shrinkage during carbonization. The suspended structures were characterized using optical and electron microscopy. Future work is to extend the characterization to wafers with different aspect ratio, and different types of mask contact during the exposure of the photoresist.

Introduction

SU-8 is an epoxy-based negative photoresist popular in the micromanufacturing industry because of its good chemical, thermal and mechanical properties (1). SU-8 is commonly used in a large number of structural applications, including lab-on-a-chip, micromolding, and microfluidics (2-6). Of particular interest here is the use of SU-8 photolithography to fabricate structures that are carbonized using a pyrolysis protocol, in a technique known as Carbon MEMS (7-10). Given an exposure mask featuring arrays of circles of varying size and gaps between them, the result of the ideal SU-8 photolithography process would be self-standing posts with no contact or interaction among them. After carbonization of such structures, the resultant shapes can be used in a number of applications; i.e. for cell manipulation using electric field gradients (11, 12). However, several authors have reported joining of the SU-8 precursor features at their top when the features are too close to each other (13-15). This effect has been deemed T-topping by some authors and has been attributed to light diffraction. The combination of light diffraction and overexposure initiates crosslinking processes of the SU-8 in zones that are covered by the opaque part of the mask, for example the area surrounding the tip of the posts. The result is an increased dimension of the cross-section compared to the theoretical value, and therefore, possible interaction between posts as the gap between them narrows. The aim of this work is to further understand this phenomena, and explore its use to fabricate suspended features between anchoring posts. Envisioned applications of these structures include wire-based sensors, structural meshes and on-chip inductors.

In this paper, we present initial results towards characterizing the impact of different parameters on the fabrication of suspended structures. We first characterized the photolithography exposure dose, followed by studying the effect of the shape and size of

the anchors and the gap between them. Shrinkage during carbonization was studied next. Lastly, the optimal parameters for the fabrication of carbon suspended bridges and wires were identified.

Materials and Methods

Arrays of structures, 5 X 5, of different dimensions and cross sections were fabricated using photolithography of SU-8 (GM1075 Gersteltec, Switzerland). A layer of 50 μm -thick was spin coated and soft baked following the recommended guidelines by the manufacturer. The exposure of the photoresist was done in a Suss MA6 Mask Aligner in soft contact mode. A parameter of study here was the time of exposure given a lamp intensity of 10 mW/cm^2 . The times studied were 10, 20, 30 and 40 s. A post-exposure bake of 25 minutes at 95 $^{\circ}\text{C}$ was implemented, followed by routine development. After developing in SU-8 developer, the structures were hard baked for 15 minutes at 190 $^{\circ}\text{C}$.

The other parameters of interest in this work were the dimensions and cross section of the structures as well as the nature of the gap between them. The cross sections studied were circles, hexagons, diamonds, squares and triangles. The dimensions of the shapes varied from 160, 80, 40, 30, 20 to 10 μm , which are either the length of one of the sides in case of polygonal shapes, or the diameter in the case of circles. The gaps studied were 45, 30, 25, 20, 15, 10 and 5 μm . The nature of the gap was one of four different cases: point-to-point (PTP), *i.e.* a triangle vertex facing another vertex; side-to-side (STS), as in two squares facing by their sides; point-to-side (PTS), when a vertex faces a flat face of its neighboring shape; and circle-to-circle (CTC), when the shapes are circular.

After fabrication, the SU-8 structures were carbonized at 900 $^{\circ}\text{C}$ for 75 minutes in a tube furnace (TF1700, Across International) in a nitrogen atmosphere; following a protocol described previously (16).

The SU-8 and carbon structures were first analyzed using optical microscopy (Nikon Eclipse LV100) and the native Nikon NIS Elements BR software. Further analysis was conducted via Scanning Electron Microscopy (SEM S3400N, Hitachi, Japan).

Results and Discussion

Upon characterization of the different structures, the following cases were identified: No Bridges (NB), Broken Bridges (BB), Stable Bridges (BB), Walls/Merged (M) and Irregular/Missing (IR). A set is defined irregular when the sets of posts are either bent against each other, bent to the ground, or just strongly deformed. We are only interested in the formation of stable bridges, which are denoted bridges or wires from this point on. When the stable bridges are wider than 1 μm they are referred to as bridges, otherwise they are classified as wires. Examples of geometries of interest are shown in Figure 1.

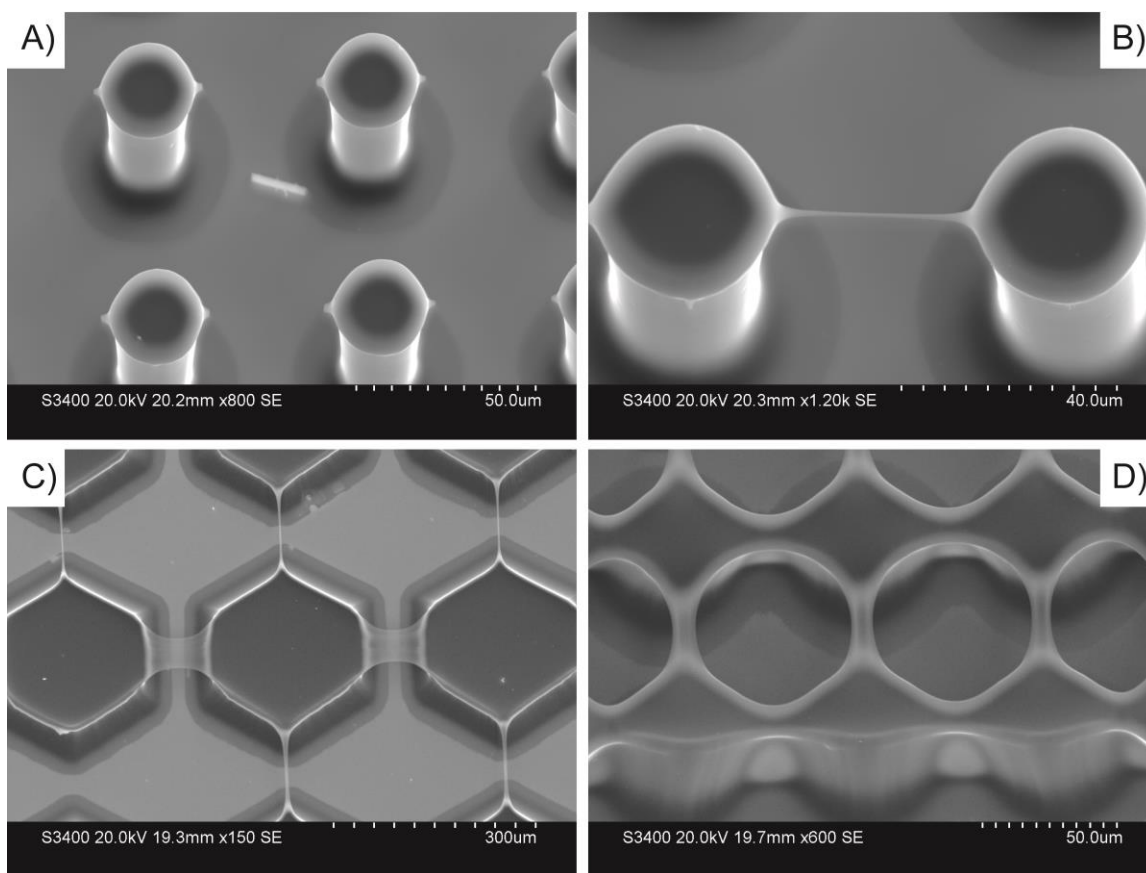


Figure 1. SEM images of: A) broken bridge; B) suspended wire; C) suspended bridge (horizontal) and wire (vertical); and D) merged posts, note how the wall extends throughout the height of the posts.

Exposure time

All the results are shown in Figure 2. The data points shown indicate the average of at least three separate measurements. The error bars are of the same dimension as the symbols and are not shown here to improve clarity when analyzing the figure. Results obtained when analyzing SU-8 structures are shown on the left (A, C, E), while results corresponding to carbon structures are shown on the right (B, D, F). The first parameter of interest was the exposure time. In this case, the type of gap was set to hexagons STS (side-to-side). The gap between two posts, the length of the side and the time of exposure were varied. Results are shown in Figures 2A-B. The y-axis details the gap size, while the x-axis includes both the length of the face (outer legends 10 to 160 μm) and the time of exposure (inner legends 10-40 s). To facilitate analysis of the results, the column related to the exposure time for each of the face lengths is presented in the same color. Stable bridges, which are the focus of this work, are denoted by stars.

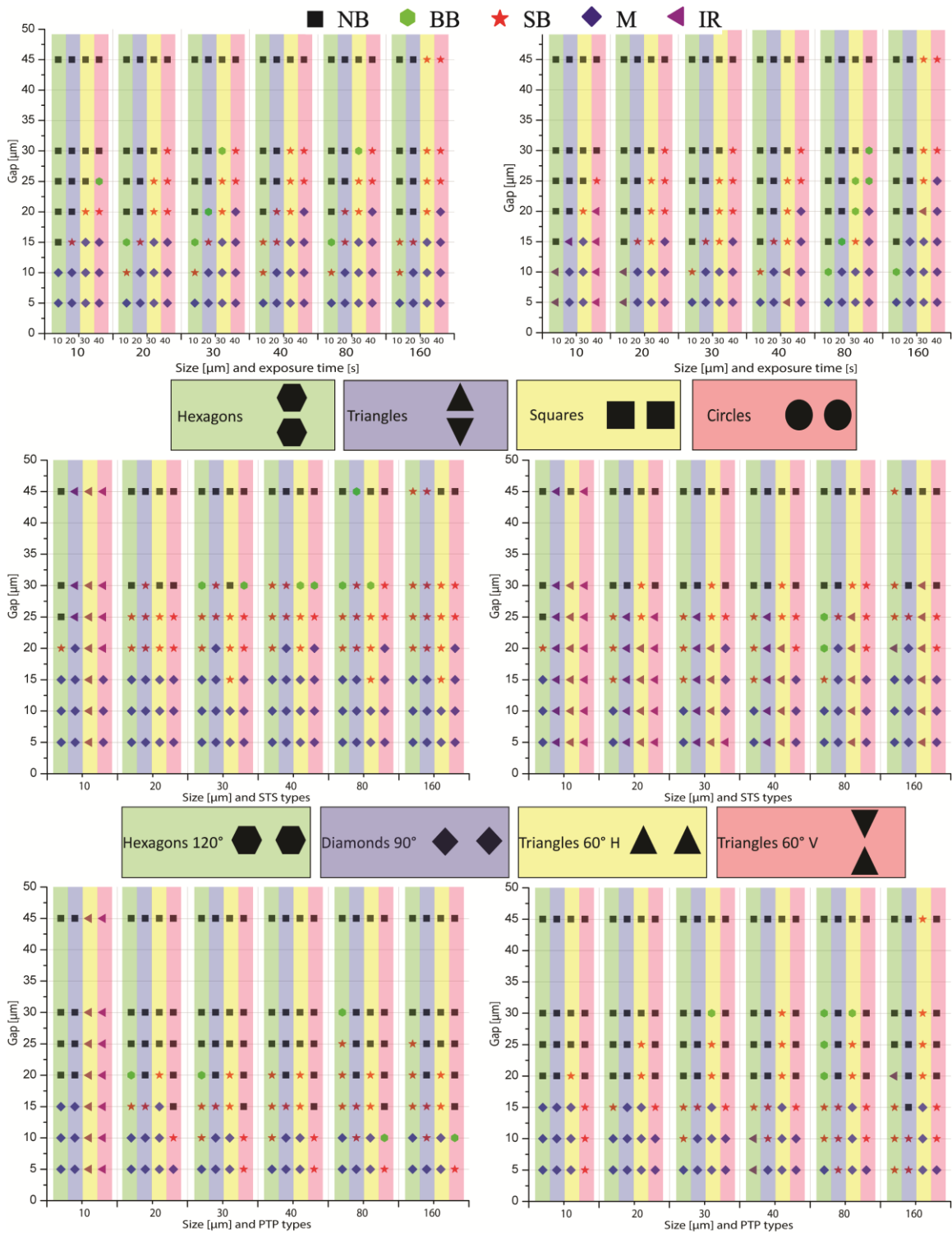


Figure 2. A) SU-8 results correlating exposure time, shape dimension and gap width when studying hexagons side-to-side; B) after carbonization of SU-8 shown in A; C) SU-8 results correlating a side-to-side gap and size of feature to the gap width for an exposure time of 30s; D) Same as C after carbonization. E) SU-8 results correlating a point-to-point gap and size of feature for an exposure time of 30s; F) results when carbonizing the structures from E.

As the time of exposure increases, the possibility to merge structures with narrow gaps increases, as well as the possibility to create stable bridges between structures with large gaps, as shown in table I.

TABLE I. Maximum gaps with stable and merged structures for hexagons STS with 80 μm side and increasing exposure time. All dimensions in μm .

Feature	Exposure 10s	Exposure 20s	Exposure 30s	Exposure 40s
Max gap with SB	10	20	25	30
Max gap with M	5	10	15	20

Conversely, a connection between two posts at low exposure times is only possible when the gap is narrow. Exposure times of 10-20 s seem the most suitable to generate wires with width around 1 μm . An expansion of the feature cross section with respect to the features in the mask was also observed with increasing exposure times. Table II gives the nominal values and the measurements taken for the shapes with characteristic dimension 160 μm , in function of the exposure time.

TABLE II. Cross section in function of the time of exposure, for different shapes with characteristic dimension 160 μm . All dimensions in μm .

Shape	Nominal size	Size for 10s	Size for 20s	Size for 30s	Size for 40s
Hexagons ¹	277.18	288	291	298	303
Triangles ²	138.5	151	155	162	165
Diamond ³	226.3	227	232	238	242.5
Squares	160	168	170	182	190
Circles	160	165	168	184	190

¹ For hexagons the measurement taken was the distance between two parallel sides.

² For triangles the measurement taken was the height.

³ For diamonds the measurement taken was the diagonal.

Size of shape

As aforementioned, different shapes with characteristic dimensions 160, 80, 40, 30, 20, 10 μm were studied. This characteristic dimension was the side length in case of a polygon and the diameter in case of a circle. It was observed that the size of a shape does not modify the trend of forming bridges. If a feature of a given size features a stable bridge (SB) for a 30 μm gap, all the other sizes of the same cross section will have a stable bridge at gap 30 μm . Although the size does not directly influence the trend of bridge formation, the dimensions of the bridges are directly proportional to the dimension of the cross section, as shown in table III.

The moment of inertia of the structures depends on the cross section and its dimensions. High aspect ratio posts with small cross sections are slender, and more inclined to bend and stick to each other in an irreversible fashion (17). This phenomenon is known as stiction, and is due to the superficial tension of the liquid meniscus that are formed in the small gaps between the posts. In this work, stiction is significant as the cross section decreases, as shown by the prevalence of irregular/missing cases in Figure 2.

TABLE III. Bridges dimensions versus cross-section size, for hexagons STS and 40s exposure. All dimensions in μm .

	Size 160 μm	Size 80 μm	Size 40 μm	Size 30 μm	Size 20 μm	Size 10 μm
Nominal gap	30	30	30	30	30	30
Average measured gap	7.64 \pm 1.37	7.47 \pm 1.33	9.19 \pm 0.6	9.3 \pm 0.71	11.47 \pm 0.56	13.81 \pm 0.63
Average measured width of structure	163.42 \pm 3.36	67.29 \pm 0.51	22.26 \pm 0.13	13.77 \pm 1.7	6.86 \pm 0.3	No Bridge

Gap type

Once the impact of the exposure time was determined we aimed at studying the effect of the gap type for a given exposure time. An exposure time of 30s was chosen because it generates stable suspended structures across many combinations of the different parameters. If the sole objective had been creating wires as thin as possible, we would have chosen 10s exposure. As detailed above, different gap types are explored: point-to-point (PTP), side-to-side (STS), point-to-side (PTS), and circle-to-circle (CTC). PTP means that the shapes are facing by points. The angle at the point is also important in order to distinguish the shapes. Shapes in this group are: hexagons (angle = 120°); triangles facing by the vertex opposite to the base (angle = 60°V); triangles facing by vertex but not aligned along the heights (angle = 60°H); diamonds (angle = 90°). STS indicates those shapes facing by a side: squares, hexagons, triangles facing by their bases. PTS occurs only in the case of triangles where one vertex faces the base of the next triangle. This type of gap is not taken in consideration, because the bridge connecting point and face is often not straight, and thus not reliable. Finally, CTC refers only to circular shapes, which have been inserted in the STS graph for simplicity. The results are shown in Figure 2C and E. Figure 2C-D shows the results obtained for fixed exposure and type of gap, 30s and STS, while varying the shape cross sections and dimensions, and gaps. Figure 2E-F show the results obtained for the same conditions of figure 2C-D but for fixed type of gap PTP.

Interaction between adjacent posts is easier when there is more material facing each other from the two sides of the connection. Thus, a STS gap will most likely have bridges at larger gaps than a PTP gap. The same observation is valid for the points with different angles; e.g, the hexagon points, which face each other with a broad angle of 120° , create bridges before the triangular points with angles of 60° . Analyzing the case of hexagonal shapes is a good way to verify this point. Comparing the first column of both graphs shown in figure 2C-E, it appears that the connection in the direction of the sides happen generally 1-2 sets earlier than in the direction of the points.

Gap width

Lastly, gap widths of 45, 30, 25, 20, 15, 10 and 5 μm were explored. The results are shown in the same figures as the gap types (fig 2C and 2E). Smaller gaps facilitate the formation of bridges. This can be confirmed looking at any column in any graph, starting

from the larger gap to the lower ones. Regardless of the type of feature there is always the ordered and general trend: no bridges to broken bridges, to stable bridges, and finally to merged posts. The explanation of this phenomenon is that, as previously discussed, light diffraction and over exposure cause an increase of the cross linked area surrounding the posts tips. For smaller gaps, these increased cross linked areas are more likely to intersect, creating a connection between the posts. The use of very small gaps eventually leads to a case of minor stiction where the posts bend towards each other. In this case, the posts curves, the tips touch each other and no suspended structure is generated. These cases were labeled as Irregular (IR) in this work and considered of no interest.

Carbonization

During the carbonization process, the SU-8 structures undergo shrinkage up to 50% of the original value. Figure 3A and B show the effect of shrinkage on four posts before and after carbonization respectively. In this case, the diameter of the posts had a contraction of about 50%, passing from an average of 93 μm to 47 μm . The suspended structures stretched from the original length of 5-6 μm up to 85-90 μm , which caused a reduction in the bridges width, and brought the vertical bridge on the left to break. The trend associated with the exposure dose in the SU-8 case structures, is maintained by the carbon structures as well. Table IV confirms that the maximum gap characterized by stable bridges and merged structures, increases with the exposure time. For the sample dimension of 40 μm , the long exposure results in bridges and merged structures at larger gaps than the short exposure

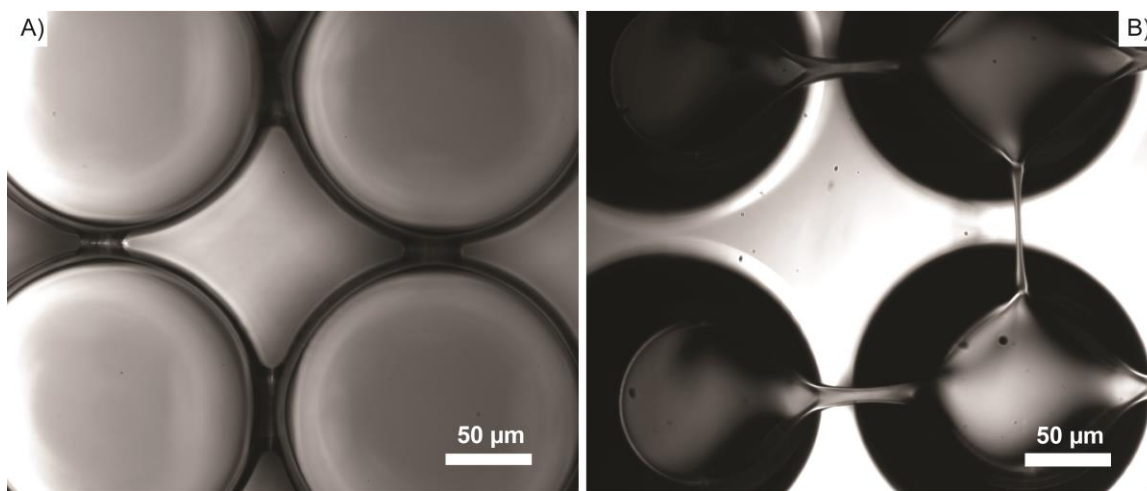


Figure 3. Circular shapes, nominal size 160 μm , nominal gap 30 μm and time of exposure 30s. A) SU-8; B) carbonized.

TABLE IV. Max gaps with stable and merged structures for hexagons STS with 40 μm side and increasing exposure time. All the dimensions are in μm .

Feature	Exposure 10s	Exposure 20s	Exposure 30s	Exposure 40s
Max gap with SB (μm)	10	15	25	30
Max gap with M (μm)	5	10	10 (IR)	20

A shift in the obtainment of usable structures can be discerned when comparing Figures 2A-B. As a direct consequence of the shrinkage, the thin structures present in the SU-8 may break under the stretching-induced stress. Nevertheless, structures that were previously merged would shrink during carbonization, leaving behind stable and thin bridges. The two counter effects can be summarized in one trend, which is a shift of the forming of structures towards lower gaps. The shift is generally limited to one gap step. As example, table V compares the value of maximum and minimum gaps with stable bridges for hexagons STS, at 30 s.

TABLE V. Value of maximum and minimum gaps with stable bridges for hexagons STS, at 30 s.

Feature	Material	Size	Size	Size	Size	Size	Size
		10 μm	20 μm	30 μm	40 μm	80 μm	160 μm
Max gap with SB (μm)	SU-8	20	25	25	30	25	45
	Carbon	20	25	25	25	15	45
Min gap with SB (μm)	SU-8	20	20	20	20	20	20
	Carbon	20	15	15	25	15	25

Analysis of the formation of bridges as a function of the type of gap, does not suggest any particular behavior that differentiates carbon from SU-8. Nevertheless, the shape and the dimension of the cross-section strongly affect the developing of cracks throughout the carbon arrays. These cracks are due to the thermal stress induced by the heat treatment and the stretching from shrinkage. Their extent is related to the quantity of material, the amount of cross-linking induced during the exposure, and the distance between two consecutive shapes. In particular, the cracking effect is the worst for bigger shapes, such as hexagons and squares, size of 160 μm , exposure of 40s, and small gaps. In general, suspended structures may be generated or not independently from the presence of cracks, but since the cracked array is not of any use, the formation of cracks indirectly affects the choice of the best process parameters.

Fabrication of carbon Wires and Bridges

The best bridges and wires characterized in this study were evaluated in terms of bridge thickness, continuity and repeatability. The optimum fabrication parameters to obtain the best suspended structures, along with the average measurements for the width and length are shown in Table VI. Wires as thin as 0.47 μm were obtained in some cases but the results were not a repeatable function of the specific process parameters. Also, the SEM characterization revealed the presence of thin nanowires ($\sim 0.01\mu\text{m}$) connecting the side walls of adjacent posts. These nanowires were not visible in the optical microscope and were not reproducible. The results of the fabrication process are shown in Figure 4A-B.

TABLE VI. Optimum fabrication parameters for wires and bridges.

Suspended Structure	Exposure time (s)	Type of gap	Size (μm)	Gap (μm)	Average width of structure (μm)	Average length of structure (μm)
Wires	10	Triangles 60°H	80	5	0.81 \pm 0.18	39.71 \pm 4.39.
Bridges	30	Hexagon STS	160	45	53.55 \pm 6.73	74.42 \pm 1.77

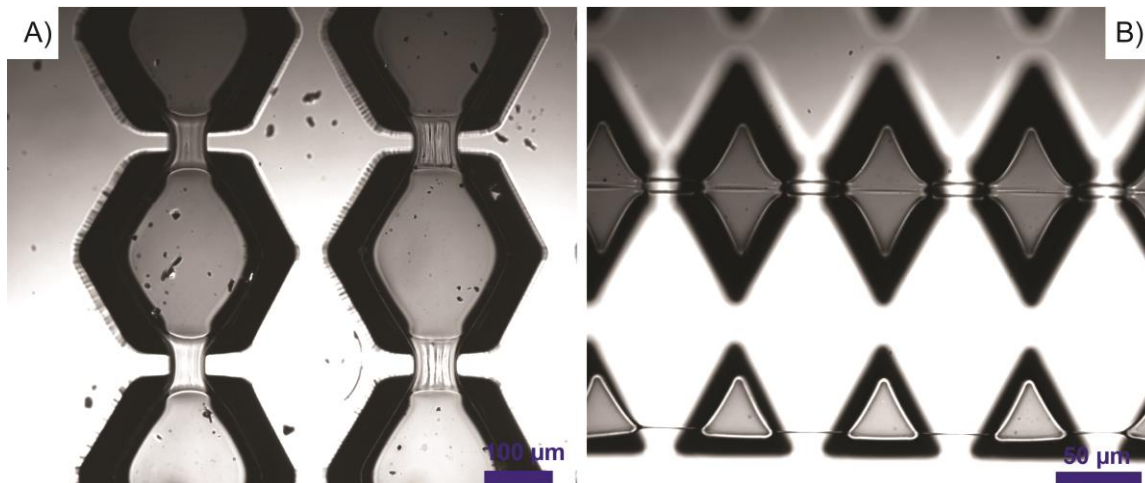


Figure 4. A) array of the optimal bridges; B) array of optimal wires.

Conclusion

In this work we have fabricated suspended carbonized wires and bridges by varying the photolithography parameters and the nature of the shapes. The process significantly depends on exposure time, gap width, and nature of the gap. The dimensions of the post anchors have some influence on the dimensions of the suspended structures. Suspended wires as thin as $0.81\mu\text{m}$ can be reproducibly obtained using low exposure time, and narrow, point-to-point gaps. In order to obtain suspended bridges, high exposure times are required. Wide bridges can be obtained with circular and squared posts but hexagonal posts facing by the sides give the best results.

Ongoing work is on determining the impact of height and other exposure modes such as hard contact and proximity mode. The goal is to enable a fabrication technique capable of making suspended carbon structures between given anchor cross sections and gap types by only optimizing the exposure setup during a normal photolithography process.

Acknowledgements

The authors would like to thank Rucha Natu for useful discussion in the formatting of some of the figures presented.

References

1. H. Lorenz, et al., *SU-8: a low cost negative resist for MEMS*, Journal of Micromechanics and Microengineering, **7**, p.121-124, (1997).
2. D. Mark, S. Haeberle, G. Roth, F. von Stetten, and R. Zengerle, *Chem. Soc. Rev.*, **39**, 1153–82 (2010).
3. T. L. Edwards, S. K. Mohanty, R. K. Edwards, C. L. Thomas, and A. B. Frazier, *Sensors Mater.*, **14**, 167–178 (2002).

4. P. Abgrall, V. Conedera, H. Camon, A. M. Gue, and N. T. Nguyen, *Electrophoresis*, **28**, 4539–4551 (2007).
5. R. Martinez-Duarte, and M. J. Madou, *Microfluidics and Nanofluidics Handbook*, 231-262 (2011).
6. R. Martinez-Duarte, *Micromachines*, **5**, 766–782 (2014).
7. B. Y. Park, L. Taherabadi, C. Wang, J. Zoval, and M. J. Madou, *J. Electrochem. Soc.*, **152**, J136 (2005).
8. S. Ranganathan, R. McCreery, S. M. Majji, and M. Madou, *J. Electrochem. Soc.*, **147**, 277 (2000).
9. J. Kim, X. Song, K. Kinoshita, M. Madou, and B. White, *J. Electrochem. Soc.*, **145**, 2314–2319 (1998).
10. B. Y. Park and M. J. Madou, *Electrophoresis*, **26**, 3745–3757 (2005).
11. W. Ma et al., *Electrophoresis*, **32**, 494–505 (2011).
12. Y. J. Chuang, F. G. Tseng, and W. K. Lin, *Microsyst. Technol.*, **8**, 308–313 (2002).
13. R. Yang and W. Wang, *Sensors Actuators, B Chem.*, **110**, 279–288 (2005).
14. S. J. Lee, W. Shi, P. Maciel, and S. W. Cha, *Proc. 15th Bienn. Univ. Ind. Microelectron. Symp. (Cat. No.03CH37488)*, 389–390 (2003).
15. A. del Campo and C. Greiner, *J. Micromechanics Microengineering*, **17**, R81–R95 (2007).
16. R. Martinez-Duarte, P. Renaud, and M. J. Madou, *Electrophoresis*, **32**, 2385–2392 (2011).
17. R. Martinez-Duarte, *Label-free Cell Sorting using Carbon Electrode Dielectrophoresis and Centrifugal Microfluidics*, PhD Mechanical & Aerospace Engineering, University of California, Irvine (2010).